On the Numerical Solution of Fields in Cavities Using the Magnetic Hertz Vector

MICHEL COUTURE

Abstract—**The possibility of using a representation of the electromagnetic fields in terms of a two-component magnetic Hertz vector to calculate fields and frequencies in cavities is examined. The governing equation is the vector Helmholtz equation, and the model is tested by calculating fields in axially symmetric cavities.**

I. Introduction

IN SOLVING Maxwell's equations numerically, one may choose to work with the integral or the differential formulation of these equations. Weiland's approach [1]–[3], based on the integral formulation and his FIT method, has been successfully applied to various problems; one of the highlights of this method has been the fact that it is free of spurious solutions. Methods based on the differential form of Maxwell's equations have also been applied successfully to many areas, such as electrostatics, magnetostatics, and eddy current problems. However, in the microwave area, the approach has encountered serious difficulties in the form of spurious solutions when attempting to solve multicomponent vector field problems in two and three dimensions [4]–[11]. It is difficult to point out the true cause (there might be several) for the occurrence of such modes. It might be that certain properties of the differential equations are not transmitted to the grid solutions or, simply, that the mathematical formulations used posssess a second set of nonphysical modes in addition to the physical ones, as was shown recently in the case of cavity problems [10]. A common characteristic of the spurious (nonphysical) resonant modes in several finite-element and finite-difference solutions of waveguides and cavities is that they do not satisfy Maxwell's magnetic divergence equation $\bar{\nabla}\cdot\bar{B}=0$. For this reason, this condition has been enforced on the solution either by a penalty method [8]–[9] or by the use of connection matrices [6]; these methods have led to reduction and, in some cases, an elimination of the spurious modes. In all of these approaches, the problem has been formulated in terms of the field components.

In the work to be described below, we report results of a study in which we have examined the possibility of using Hertz potentials to solve Maxwell's equations numerically; the problem considered was that of empty cavities. Although Hertz's potentials have proven useful [12]–[19] in the analysis of waveguides and microstrips, the possibility of using them in a numerical calculation has not been much explored. By introducing Hertz potentials, one reduces the number of differential equations to solve while satisfying some of Maxwell's equations identically; for instance, one is assured that $\bar{\nabla}\cdot\bar{B}=0$ will be satisfied. Another motivating factor in studying these potentials is that by appropriately choosing the gauge, any three-dimensional electromagnetic field in vacuum can be represented by a two-component Hertz vector. However, there are problems associated with the use of such potentials in a numerical calculation, one of which is more complicated boundary conditions; also, since these are gauge fields, one faces the problem of gauge fixing.

The representation considered had the following features.

1) The electromagnetic fields are expressed in terms of the magnetic Hertz vector $\bar{\pi}_m$, where $\bar{\pi}_m$ is perpendicular to the z-axis.

2) The vector $\bar{\pi}_m$ satisfies the homogeneous vector Helmholtz equation.

3) In the case of angle-independent modes in axially symmetric cavities, this representation leads to a formulation in terms of a single variable $\pi_{m\theta}$ (in this particular case, $\pi_{m\theta}$ is proportional to B_θ), and the governing eqution is the generalized Bessel equation [20] of order one, which is the governing equation (or the Euler equation) of existing codes designed to do such calculations [21], [25].

The above representation has been tested by using it to calculate modes in axially symmetric cavities; as cavity problems are concerned, this is the simplest case of a multicomponent vector field problem. Since the formulation considered lends itself very well to the techniques used in the SUPERFISH [21] code, we modeled our approach on the one used in that code. This approach can be seen as a generalization of SUPERFISH without the singularities encountered in ULTRAFISH [22].

The paper is divided as follows. In Section II we briefly recall some known results on Hertz vectors and their gauge transformation. In Section III, a formulation of the electromagnetic fields in terms of the magnetic Hertz vector is presented, and the remaining gauge invariance in this representation is discussed; means of fixing the gauge are proposed. In Section IV, the case of a cylindrical cavity is solved analytically in this particular gauge. In Section V, the discretization method chosen is presented. Finally, in Section VI, results are discussed and compared with analytical solutions, measured values, and results from

Manuscript received June 17, 1986; revised October 8, 1986.

The author is with the Theoretical Physics Branch, Chalk River Nuclear Laboratories, Chalk River, Ontario, Canada, K0J 1J0.

IEEE Log Number 8612435.

URMEL [1] and ULTRAFISH [22] for several cavities and modes. MKS units are assumed throughout.

II. Hertz's Vectors and Their Gauge Transformation

In the absence of charges and currents, any electromagnetic field may be expressed in terms of two Hertz vectors as follows [23]–[24]

$$\bar{E} = \bar{\nabla}(\bar{\nabla} \times \bar{\pi}_e) - \frac{1}{c^2}\frac{\partial^2}{\partial t^2}\bar{\pi}_e - \mu_0 \frac{\partial}{\partial t}(\bar{\nabla} \times \bar{\pi}_m)$$

$$\bar{B} = \frac{1}{c^2}\frac{\partial}{\partial t}(\bar{\nabla} \times \bar{\pi}_e) + \mu_0 \bar{\nabla} \times \bar{\nabla} \times \bar{\pi}_m \tag{1a}$$

where $\bar{\pi}_e$ and $\bar{\pi}_m$ both satisfy the homogeneous vector Helmholtz equation

$$\nabla^2 \bar{\pi} - \frac{1}{c^2}\frac{\partial^2}{\partial t^2}\bar{\pi} = 0. \tag{1b}$$

The vectors $\bar{\pi}_e$ and $\bar{\pi}_m$ are not uniquely defined. In fact, there are an infinite number of possible sets $\bar{\pi}_e$ and $\bar{\pi}_m$ for a given electromagnetic field. This high multiplicity can be understood in terms of the following gauge transformations [24]:

$$\bar{\pi}_e \to \bar{\pi}_e' = \bar{\pi}_e + \bar{\nabla} \times \bar{\Gamma} - \mu_0 \frac{\partial \bar{\Lambda}}{\partial t} - \bar{\nabla}\lambda$$

$$\bar{\pi}_m \to \bar{\pi}_m' = \bar{\pi}_m - \epsilon_0 \frac{\partial \bar{\Gamma}}{\partial t} - \bar{\nabla}\gamma - \bar{\nabla} \times \bar{\Lambda} \tag{2}$$

where, for the case considered here, λ, γ, $\bar{\Gamma}$, and $\bar{\Lambda}$ satisfy (1b). The above gauge transformations allow one to represent any electromagnetic field in vacuum in several ways. We shall now discuss a representation in terms of the magnetic vector $\bar{\pi}_m$.

III. A Representation in Terms of a Single Vector $\bar{\pi}_m$

The representation considered in this paper is the following:

$$\bar{E} = -\mu_0 \frac{\partial}{\partial t}(\bar{\nabla} \times \bar{\pi}_m) \quad \bar{B} = \mu_0 \bar{\nabla} \times \bar{\nabla} \times \bar{\pi}_m$$

$$\bar{\pi}_m = (\pi_{mr}, \pi_{m\theta}, 0) \tag{3}$$

where $\bar{\pi}_m$ satisfies the vector Helmholtz equation (1b). The representation (3) is obtained from the one given in (1) by gauge transformations [23]. A first step consists in eliminating $\bar{\pi}_e$ by appropriately choosing $\bar{\Lambda}(\bar{\Gamma}, \lambda, \gamma = 0)$ in (2). Then one can always define a $\gamma(\bar{\Gamma}, \bar{\Lambda}, \lambda = 0)$ such that following this transformation $\bar{\pi}_m$ is perpendicular to the z-axis. In cylindrical coordinates, one may verify that the only possible choice leading to a general field representation and a homogeneous vector Helmholtz equation is the elimination of the z-component of $\bar{\pi}_m$. In Cartesian coordinates, one may choose to eliminate any one of the three components of $\bar{\pi}_m$ and still have a representation for a general electromagnetic field with $\bar{\pi}_m$ satisfying the homogeneous vector Helmholtz equation.

Even within the gauge (3), $\bar{\pi}_m$ is not uniquely defined for a given $\bar{E}$ and $\bar{B}$. In fact, one can always add to $\bar{\pi}_m$ a vector $\bar{Z}$ which is perpendicular to the z-axis and satisfies the following equations:

$$\bar{\nabla} \times \bar{Z} = 0 \quad \nabla^2 \bar{Z} - \frac{1}{c^2}\frac{\partial^2}{\partial t^2}\bar{Z} = 0. \tag{4a}$$

Thus

$$\bar{Z} \equiv (f^*, f, 0) \tag{4b}$$

where $f(r, \theta, t)$ and $f^*(r, \theta, t)$ are functions which do not depend on z. $\bar{Z}$ will be referred to as the zero-field solution since it satisfies the vector Helmholtz equation as well as the boundary conditions but contributes nothing to the fields $\bar{E}$ and $\bar{B}$. Equations (4) express the remaining gauge freedom in the representation (3) for a general three-dimensional problem. Assuming a $\cos(\omega t)$ time dependence for $\bar{\pi}_m$, let us solve for $\bar{Z}$ in the case of axially symmetric problems.

In the case of angle-independent modes, one may verify that the components of $\bar{\pi}_m$ are decoupled. TM modes are expressed in terms of $\pi_{m\theta}$, and TE modes in terms of π_{mr}. In the case of TM modes $f = 0$, and denoting the spatial part of $\pi_{m\theta}$ by $\phi(r, z)$ and the θ-component of the magnetic field by B_θ, we have that $B_\theta = \mu_0 k^2 \phi$, where $k \equiv \omega/c$; in that case, solving the problem in terms of the Hertz component $\pi_{m\theta}$ is equivalent to solving it in terms of B_θ. In the case of TE modes, some gauge freedom remains since $f^* \neq 0$; however, one need not worry about gauge fixing since the best way to calculate these modes is to treat them as TM modes (using ϕ as the variable), with the difference that metallic surfaces are now considered as magnetic ones ($\phi = 0$) and magnetic ones as metallic surfaces; the values of B_θ, E_r, and E_z obtained are then interpreted as those of E_θ, B_r, and B_z, respectively.

We now turn to the angle-dependent modes and assume the following spatial and time dependence:

$$\pi_{mr}(r, \theta, z, t) = \frac{\Psi^*(r, z)}{r} \sin(m\theta)\cos(\omega t)$$

$$\pi_{m\theta}(r, \theta, z, t) = \frac{\Psi(r, z)}{r} \cos(m\theta)\cos(\omega t)$$

$$f^*(r, \theta, t) = \frac{G^*(r)}{r} \sin(m\theta)\cos(\omega t)$$

$$f(r, \theta, t) = \frac{G(r)}{r} \cos(m\theta)\cos(\omega t). \tag{5}$$

Solving (4) and demanding that on the axis $\Psi = 0$ and $\Psi^* = 0$, we get after some analysis for $m \neq 0$

$$G(r) = AJ_m(kr), \quad G^*(r) = A\frac{r}{m}\frac{\partial}{\partial r}J_m(kr) \tag{6}$$

where A is some arbitrary constant which we will refer to as the gauge constant. The gauge-fixing problem has therefore been narrowed down to fixing one scalar constant, A.

In using representation (3) in a numerical calculation, one must specify not only the normalization (as we do through (17)) but also the value of A. Equations (6)

suggest that the gauge could be fixed by requiring that at almost any off-axis point $P = (r_0, z_0)$

$$\Psi = c_1 \text{ or } \Psi^* = c_2 \tag{7}$$

where c_1 and c_2 are arbitrary constants which could also be set to zero; (7) is always possible provided kr_0 is not a zero of J_m or of $\partial J_m/\partial r$. Another option exists if there are magnetic symmetry planes; one may verify that on such planes ($z =$ constant) the r dependence of Ψ and Ψ^* is exactly that of G and G^*, so that one may fix the gauge by demanding that on one of these planes

$$\bar{\pi}_m = 0. \tag{8}$$

Let us conclude this section with a few remarks. First, we note that eqs. (4) are not sufficient to determine $\bar{Z}$ uniquely for a given frequency. For example, in the axially symmetric case, the general solution of (4) is $G(r) = AJ_m(kr) + DY_m(kr)$, where D is some arbitrary constant; by setting $\Psi = 0$ and $\Psi^* = 0$ on the axis, we are actually setting $D = 0$. Second, we stress the fact that $\bar{Z}$ satisfies (1b) as well as the boundary conditions (since $\bar{\nabla} \times \bar{Z} = 0$) for *all* frequencies. The formulation given in (3) has therefore two types of solutions: the physical solutions, whose frequency spectrum is discrete, and the zero-field solutions, whose spectrum is continuous, the latter being a manifestation of the remaining gauge freedom in the formulation (3). The method of fixing the gauge proposed in (8) would in fact exclude all zero-field solutions. In the case of (7), by appropriately choosing r_0, one could also exclude the zero-field solutions. These gauge-fixing methods were proposed with the assumption that the remaining gauge freedom as expressed in (4) and (6), being an analytical property of the differential equations, would be transferred to the grid solution. But is this assumption correct? Since the existence of the gauge invariance is linked to the existence of solutions whose spectrum is continuous, the answer is not obvious. In Section VI, we shall look into this problem through several examples, one of which will be the cylindrical cavity since it is the simplest one to solve analytically.

IV. Analytical Solutions for a Cylindrical Cavity

The solution given in this section pertains to the cylindrical cavity shown in Fig. 1. Only one quarter of an azimuthal cross section of the cavity is shown, the radius being R and the length $2L$. Sides AA' and BA are metallic surfaces and BB' is a metallic symmetry plane.

Solutions for TM_{mnp} modes with $m \neq 0$ are given in (9). These were obtained by first solving in the gauge for which $\bar{\pi}_m = 0$ and $\bar{\pi}_e = (0, 0, \pi_{ez})$; then, solutions in the gauge (3) were obtained through a gauge transformation. For TM modes, we get

$$\pi'_{mr} = \left[-\frac{mN}{kr} J_m(\tau_{mn} r) \cos\left(\frac{p\pi}{L} z\right) + \frac{A}{m} \frac{\partial J_m(kr)}{\partial r} \right] \sin(m\theta) \cos(\omega t)$$

$$\pi'_{m\theta} = \left[-\frac{N}{k} \frac{\partial J_m(\tau_{mn} r)}{\partial r} \cos\left(\frac{p\pi}{L} z\right) + \frac{A}{r} J_m(kr) \right] \cos(m\theta) \cos(\omega t) \tag{9}$$

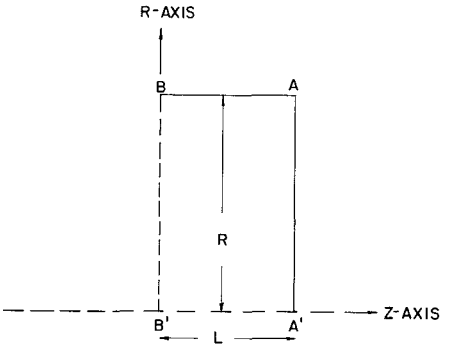

Fig. 1. Cylindrical cavity.

with

$$\tau_{mn} = \frac{x_{mn}}{R} \quad p = 0, 1, 2, \cdots$$

where x_{mn} is the nth root of J_m; N is some arbitrary normalization constant whose value is determined by the position of the driving point (see Section V-D) through (17); and A is the gauge constant.

A similar procedure is followed for TE_{mnp} modes; for $m \neq 0$, we get

$$\pi'_{mr} = \left[\frac{N}{p} \frac{L}{\pi} \frac{\partial J_m(\tau'_{mn} r)}{\partial r} \cos\left(\frac{p\pi}{L} z\right) + \frac{A}{m} \frac{\partial J_m(kr)}{\partial r} \right] \cdot \sin(m\theta) \cos(\omega t)$$

$$\pi'_{m\theta} = \left[\frac{mNL}{p\pi} \frac{J_m(\tau'_{mn} r)}{r} \cos\left(\frac{p\pi}{L} z\right) + \frac{A}{r} J_m(kr) \right] \cdot \cos(m\theta) \cos(\omega t) \tag{10}$$

where

$$\tau'_{mn} = \frac{x'_{mn}}{R} \quad p = 1, 2, 3, \cdots$$

and x'_{mn} is the nth root of $\partial J_m/\partial r$. Solutions for cases having one or two magnetic symmetry planes are obtained in a similar way.

V. Discretizing the Problem

A. Governing Equations

We now proceed to discretize the problem in the representation (3). Assuming the angle and time dependence given in (5), the set of differential equations to be discretized is

$$\frac{1}{r} \frac{\partial^2 \Psi^*}{\partial r^2} + \frac{1}{r} \frac{\partial^2 \Psi^*}{\partial z^2} - \frac{1}{r^2} \frac{\partial \Psi^*}{\partial r} + \left(\frac{k^2}{r} - \frac{m^2}{r^3} \right) \Psi^* + \frac{2m}{r^3} \Psi = 0 \tag{11}$$

and

$$\frac{1}{r}\frac{\partial^2\Psi}{\partial r^2}+\frac{1}{r}\frac{\partial^2\Psi}{\partial z^2}-\frac{1}{r^2}\frac{\partial\Psi}{\partial r}+\left(\frac{k^2}{r}-\frac{m^2}{r^3}\right)\Psi+\frac{2m}{r^3}\Psi^*=0. \quad (12)$$

The method of solution that we shall now briefly describe is modeled on the one used in the SUPERFISH code. We also used SUPERFISH's triangular mesh generator; each mesh point is surrounded by six triangles. Difference equations are obtained by the weighted residual method. In order to generate contour integrals through which boundary conditions will be imposed, some algebraic manipulations are needed. Essentially by adding and subtracting the same terms on the left-hand sides of (11) and (12) but changing the order of differentiation (for instance, $\partial/\partial z(\partial\Psi^*/\partial r)$ and $\partial/\partial r(\partial\Psi^*/\partial z)$, one is able to generate the appropriate contour integrals. The procedure is therefore as follows. In order to avoid singularities on the axis, we first multiply the left-hand sides of (11) and (12) by r^3; after the algebraic manipulations mentioned above, we follow Winslow's [26] approach and integrate over the portion Ω of the area of the dodecagon (see Fig. 2) which is in the problem area. The vertices of the dodecagon are alternatively the centroids of the six adjacent triangles and the midpoints of the six adjacent sides, as shown in Fig. 2. For interior points, Ω is the total area of the dodecagon surrounding the mesh point. For boundary points, Ω is only a fraction of the total area. For example, let us consider a boundary going through points (M is the mesh point) 4-M-10. One possibility is that Ω would be the area of the polygon whose corner points are 4-5-6-7-8-9-10-M; the other possibility is for Ω to be defined as the area of the polygon whose corner points are 10-11-12-1-2-3-4-M. Using Green's theorem to reduce the order of differentiation, the governing integral equations are

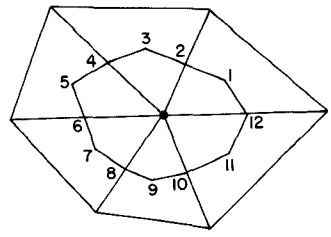

Fig. 2. Dodecagon region of integration.

where $d\bar{s}=ds\hat{t}$, ds being an element of length of the perimeter C of Ω and $\hat{t}$ a unit vector tangential to C; $\hat{r}$ and $\hat{z}$ are unit vectors along the r- and z-axes. Discretization is carried out by assuming that Ψ and Ψ^* are linear functions of r and z within each triangle.

B. Boundary Conditions

On metal surfaces, the boundary conditions are

$$E_\theta=0\rightarrow\frac{\partial\Psi^*}{\partial z}=0 \quad (15a)$$

and

$$\bar{E}\cdot d\bar{s}=0\rightarrow\bar{\nabla}\times\bar{\pi}_m\cdot d\bar{s}=0\rightarrow\left(-r^2\frac{\partial\Psi}{\partial z}\hat{r}+r^2\frac{\partial\Psi}{\partial r}\hat{z}-mr\Psi^*\hat{z}\right)\cdot d\bar{s}=0. \quad (15b)$$

On magnetic surfaces (these are symmetry planes where $z=$ constant), boundary conditions may be expressed as follows:

$$B_\theta=0\rightarrow\frac{m}{r^2}\left(\frac{\partial\Psi^*}{\partial r}-m\frac{\Psi}{r}\right)+k^2\frac{\Psi}{r}=0 \quad (16a)$$

$$B_r=0\rightarrow\frac{\partial\Psi}{\partial r}-m\frac{\Psi^*}{r}=0. \quad (16b)$$

The boundary condition (15b) is imposed through the first contour integral of (13); this is done by omitting the contribution to the contour integral of the section of C which is along the metal surface. Boundary conditions (16a) and (16b) are imposed in the same way through the second contour integrals of (14) and (13), respectively. (This method of imposing boundary conditions is a standard one in finite elements and is the one used in the SUPERFISH program.) For the boundary condition (15a), no efficient analogous procedure was found; we therefore imposed it explicitly. Finite-difference methods for arbitrary meshes have been the subject of many studies [31]–[35]. The method we have used to obtain a finite-dif-

$$\oint_{\hat{C}}\left[\left(-r^2\frac{\partial\Psi}{\partial z}\hat{r}+r^2\frac{\partial\Psi}{\partial r}\hat{z}-mr\Psi^*\hat{z}\right)\right]\cdot d\bar{s}+\oint_{\hat{C}}r^2\left(\frac{\partial\Psi}{\partial r}-m\frac{\Psi^*}{r}\right)\hat{r}\cdot d\bar{s}+\oint_C r^2\frac{\partial\Psi}{\partial z}\hat{z}\cdot d\bar{s}-\int_\Omega\left[(k^2r^2-m^2)\Psi+mr\frac{\partial\Psi^*}{\partial r}-3\left(r\frac{\partial\Psi}{\partial r}-m\Psi^*\right)-2r\frac{\partial\Psi}{\partial z}-mr\frac{\partial\Psi^*}{\partial z}\right]d\Omega=0 \quad (13)$$

and

$$\oint_{\hat{C}}\left[\left(-r^2\frac{\partial\Psi^*}{\partial z}\hat{r}+r^2\frac{\partial\Psi^*}{\partial r}\hat{z}-mr\Psi\hat{z}\right)+mr^2\frac{\partial\Psi^*}{\partial z}\hat{z}\right]\cdot d\bar{s}+\oint_{\hat{C}}\left[r^4\left(\frac{m}{r^2}\frac{\partial\Psi^*}{\partial r}-\frac{m^2\Psi}{r^3}+\frac{k^2\Psi}{r}\right)\hat{r}\right]\cdot d\bar{s}-\int_\Omega\left[(k^2r^2-m^2)\Psi^*+mr\frac{\partial\Psi}{\partial r}-3\left(r\frac{\partial\Psi^*}{\partial r}-m\Psi\right)+r(k^2r^2-m^2)\frac{\partial\Psi}{\partial z}-2mr\frac{\partial\Psi^*}{\partial z}\right]d\Omega=0 \quad (14)$$

TABLE I
MODES: 0–9000 MHz. CAVITY: CYLINDER (FIG. 1).

Modes	Analytical Frequencies (MHz)	Calculated Frequencies (MHz)			
		280 mesh points		760 mesh points	
		A = 0	A ≠ 0	A = 0	A ≠ 0
ZERO			1044.62		
ZERO			3659.10		
TE_{211}	4802.57	4799.95(+2.62)	4799.86(+2.71)	4801.45(+1.12)	4801.31(+1.26)
TM_{210}	4900.76	4892.02(+8.74)	4892.65(+8.11)	4897.96(+2.8)	4898.23(+2.53)
TM_{211}	6211.88	6205.27(+6.61)	6208.08(+3.8)	6209.73(+2.15)	6209.68(+2.2)
ZERO			6559.74		
TE_{221}	7451.37	7426.55(+24.82)	7421.70(+29.67)	7441.10(+10.27)	7440.09(+11.28)
TM_{220}	8032.31	8011.26(+21.05)	8012.18(+20.13)	8027.10(+5.21)	8027.19(+5.12)
TE_{212}	8171.58	8191.85(-20.27)	8214.99(-43.41)	8179.20(-7.62)	8184.11(-12.53)
TM_{221}	8893.15	8876.86(+16.29)	8877.92(+15.23)	8889.11(+4.04)	8889.02(+4.13)

ference expression for the derivative was based on the least-square principle and was applied to the irregular triangular mesh of the SUPERFISH code. This technique has already been the object of some studies [36], [37]. The method we used is similar to the one used in the COMPELL [38] code and therefore will not be discussed here.

C. System of Equations

Following discretization, we end up with a tridiagonal block system of equations which we solve, as in SUPERFISH [21], by a Gaussian block elimination process.

D. Driving Current

The discretization procedure leads to a set of homogeneous difference equations. As in SUPERFISH, an inhomogeneous term is introduced on the right-hand side of this system of equations by demanding that at a given mesh point (driving point)

$$B_\theta = 1 \text{ or } B_r = 1. \tag{17}$$

At this point, it should be mentioned that the analysis leading to (3) remains valid even in the presence of fictitious magnetic charges and currents (driving current). Because of that, resonant frequencies have been found by using a root-finding algorithm modeled on the one used in the SUPERFISH code.

VI. TEST CASES

One of the objectives of the tests we are about to describe was to examine the problem of gauge fixing. Is the gauge freedom described in Section III transferred to the grid solution? If this is the case, then one would have to fix the gauge as suggested in (7) or (8) in order to get a unique solution for a given physical mode. The other objective was obviously to verify the accuracy with which eigenfrequencies could be calculated. Tests [23] were done with several geometries and modes; only some of these results are given here.

A. Modes of a Cylinder

All $m = 2$ modes up to 9000 MHz were calculated with 280 and 760 mesh points for the cylindrical cavity shown in Fig. 1 (boundaries BB' and AA' were considered metallic surfaces and $R = 5$ cm, $L = 3.927$ cm). We first calculated these modes by imposing that $\Psi^* = 0$ ($c_2 = 0$ in (7)) on the upper boundary BA; numerical results agreed very well with the analytical ones given in (9) and (10) with $A = 0$. Results are shown in Table I in the columns headed $A = 0$. The same modes were then calculated without fixing the gauge. Here, (15a) is imposed instead of $\Psi^* = 0$ along BA; again, numerical and analytical values agreed very well but this time with $A \neq 0$. Results are shown in Table I in the columns headed $A \neq 0$. Physical modes have therefore been calculated in two different gauges.

A first observation is that in all cases given in the columns headed $A \neq 0$, the gauge has been fixed through the discretization process. A second observation is that resonant modes (ZERO) found which did not correspond to physical modes were actually zero-field solutions. Numerical results agreed very well with the analytical solutions given in (6); zero modes were not observed with 760 mesh points. However, we cannot exclude the possibility of having missed them, although we have looked through the whole 9000-MHz spectrum by steps of 50 MHz. Before going any further, it must be said that we do not have a complete understanding of how the truncation errors associated with discretization manage to fix the gauge; however, we did observe that the values of the gauge constant varied with the mesh size and the discretization method used for boundary conditions. We believe that the type of mesh used (triangular, rectangular, $\cdots$) would also be a

factor contributing in fixing the value of A. Although we were successful in fixing the gauge for a cylinder, for more complicated geometries the methods proposed in (7) and (8) prove to be less successful; we believe that since the gauge is being fixed through the discretization process, by attempting to impose (7) or (8) we might be overspecifying the problem. The conclusion is therefore that there is no need to fix the gauge since it is being fixed through the discretization process.

B. Cavities of Complex Shape

Let us now consider the Mainz cavity shown in Fig. 3. This cavity is used in the microtron at the University of Mainz and has a $\pi/2$ TM_{010} mode frequency of 2.45 GHz. It is an on-axis-coupled cavity. In Table II, results [27] from the URMEL code [1] and our code (HERTZ) are compared with measured values [28].[1] All modes are dipole modes ($m=1$). On the right-hand side of this table, the boundary condition on planes AA' and BB' are given; M stands for a magnetic surface and E for a metallic one. In both cases, approximately 700 mesh points were used. For magnetic surfaces, we have considered two cases: in one case the gauge was fixed through the discretization process, in the other (results shown in parentheses), the problem was solved in the gauge satisfying (8). For all the other modes, the gauge was fixed through the discretization process.

Finally, we consider the cavity shown in Fig. 4; this is the PIGMI $\beta=.8$, frequency = 2380 MHz cavity. In Table III, results [27] from the URMEL, ULTRAFISH [29], and our own code are compared with measured values [29]; some of the experimental values are not measured but extrapolated from measured points, since some modes are forbidden by end plates; these values are preceded by $\simeq$ (this remark concerning extrapolated values was taken from Iwashita's technical note [29]). Boundary conditions are indicated as in Table II. Here again, differences between measured and calculated frequencies are shown in parentheses. In all cases, the gauge was fixed through the discretization process.

Let us conclude this section with a few remarks. When using gauge fields in a numerical calculation, one faces the problem of uniqueness. The use of the magnetic vector potential $\bar{A}$ for the numerical solution of three-dimensional problems in magnetostatics has initiated, in the last few years, several studies concerning the uniqueness problem [39]–[40]; central to this question is the specification of the divergence of $\bar{A}$. As we have shown in this paper, when using Hertz potential for cavity problems, the question of uniqueness presents itself differently. The methods suggested in (7) or (8) were also meant to ensure uniqueness. However, as our results showed, these proved unnecessary; in fact, in some cases one might be overspecifying the problem by imposing such conditions. As a consequence of discretization, the zero-field spectrum is no longer continuous; nonuniqueness can only occur if a resonant zero mode coincides with a resonant physical mode. Our results suggest that this never occurs. If it did happen, the methods proposed in (7) or (8) would remove the numerical difficulty. We had expected that by decreasing the mesh size the number of zero modes would increase since we are, in fact, approximating a solution (the zero-field) whose spectrum is continuous. However, results given

TABLE II
MAINZ CAVITY

Measured (MHz)	URMEL (MHz)	HERTZ (MHz)	Boundary Conditions plane AA'	plane BB'
4179.	4178.(+1.)	4180.(-1.)	E	E
5892.	5909.(-17.)	5915.(-23) (5906.)	M	E
6785.	6704.(+81.)	6702.(+83.)	E	E
8262.	8130.(+132.)	8130.(+132.) (8115.)	M	E
11215.	11169.(+46.)	11232.(-17.)	E	E

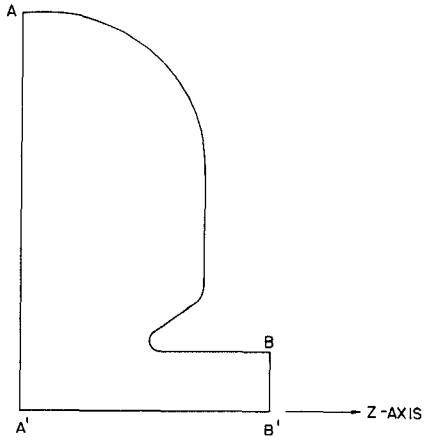

Fig. 3. Mainz cavity.

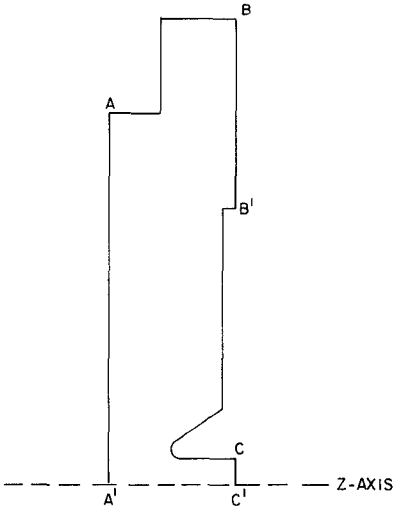

Fig. 4. PIGMI cavity.

[1] The modes we used for comparison are the ones which, according to the authors of these measurements (H. Herminghaus and H. Enteneuer), were believed to be the most accurately measured (private communication from K. C. D. Chan).

TABLE III
PIGMI CAVITY

Mode	Measured (MHz)	URMEL (MHz)	ULTRAFISH (MHz)	HERTZ (MHz)	Boundary Conditions	
					plane AA'	plane BB' and CC'
TM_{110}	2102.5	2096(+7)	2110.0(-8)	2093.9(+9)	E	E
$TM_{11\pi}$	≈2500	2462(+38)	2496.3(+4)	2493.5(+6)	M	E
TE_{110}	≈760	777(-17)	775.2(-15)	768.6(-9)	M	M
$TE_{11\pi}$	1299.3	1290(+9)	1314.6(-15)	1289.5(+10)	E	M
TM_{210}	2765.1	2752(+13)	2767.3(-2)	2761.4(+4)	E	E
$TM_{21\pi}$	≈2800.	2759(+41)	2790.9(+9)	2790.4(+10)	M	E
TE_{210}	≈1540.	1544(-4)	1540.0(0)	1528.9(+10)	M	M
$TE_{21\pi}$	2117.6	2101(+17)	2133.8(-16)	2112.4(+5)	E	M
TE_{310}	≈2280.	2298(-18)	2290.9(-11)	2289.8(-10)	M	M
$TE_{31\pi}$	2894.1	2875(+19)	2918.5(-24)	2884.1(+10)	E	M

in Table I do not confirm this expectation; more cases need to be studied before drawing any firm conclusion on this particular point. Finally, let us add that gauge fixing through discretization has also been reported with a model based on the magnetic vector potential for the solution of 3-D eddy current problems [30].

VII. Conclusions

In this paper, a solution of the cavity problem in terms of a two-component magnetic Hertz vector has been examined; empty cavities were considered. The main difficulty associated with the use of such a representation in a numerical calculation is that of gauge fixing. Analytically, we have shown that for both two- and three-dimensional problems, the physical solution is defined only within a zero-field solution whose frequency spectrum is continuous. In order to study what happens in the grid space, we have used the model to solve the problem of axially symmetric cavities. The main results are as follows.

1) Results obtained are good. We believe that the accuracy of frequencies could be increased by improving the least-square method used to approximate one of the boundary conditions ($E_\theta = 0$).

2) The gauge is fixed by the discretization procedure. This can be understood from the observation that following discretization the spectrum of zero-field solutions is discrete; the gauge invariance is not carried over to the grid space.

3) The vector Helmholtz equation has been solved without any constraints; as for boundary conditions, only the tangential components of the electric (on metallic surfaces) and of the magnetic (on magnetic surfaces) fields were required to be zero.

4) The only nonphysical resonant modes found were easily identified as zero-field solutions.

In the light of the results obtained for the two-dimensional case, we expect that if applied to three-dimensional problems the gauge would also be fixed through the discretization procedure with zero-field solutions as the only nonphysical modes. Although results are encouraging, it is clear that in order for a Hertz potential formulation to become an effective alternative to field-component formulations, more work needs to be done. The process by which the gauge is fixed through the discretization procedure needs to be better understood; it also remains to be discovered whether these zero modes can be eliminated by imposing some sort of constraint.

Acknowledgment

The author would like to thank G. E. Lee-Whiting for many helpful discussions. He would also like to thank K. C. D. Chan for allowing him to use the results of his tests of the URMEL code.

References

[1] T. Weiland, "On the computation of resonant modes in cylindrical symmetric cavities," *Nucl. Instrum. Methods*, vol. 216, pp. 329–348, 1983.

[2] T. Weiland, "On the numerical solution of Maxwell's equations and applications in the field of accelerator physics," *Part. Accel.*, vol 15, pp. 245–292, 1984.

[3] T. Weiland, "Three dimensional resonator mode computation by finite difference method," *IEEE Trans. Magn.*, vol. MAG-21, pp. 2340–2343, Nov. 1985.

[4] A. Konrad, "Triangular finite elements for vector fields in electromagnetics," Ph.D. thesis, McGill University, Montreal, Canada, 1975.

[5] A Konrad, "Vector variational formulation of electromagnetic fields in anisotropic media," *IEEE Trans. Microwave Theory Tech.*, vol. MTT-24, pp. 553–559, Sept. 1976.

[6] A. Konrad, "A direct three-dimensional finite element method for the solution of electromagnetic fields in cavities," *IEEE Trans. Magn.*, vol. MAG-21, pp. 2276–2279, Nov. 1985.

[7] J. B. Davies, F. A. Fernandez, and G. Y. Philippou, "Finite element analysis of all modes in cavities with circular symmetry," *IEEE Trans. Microwave Theory Tech.*, vol MTT-30, pp. 1975–1980, Nov. 1982.

[8] B. M. A. Rahman and J. B. Davies, "Penalty function improvement of waveguide solution by finite elements," *IEEE Trans. Microwave Theory Tech.*, vol. MTT-32, pp. 922–928, Aug. 1984.

[9] M. Hara, T. Wada, T. Fukasawa, and F. Kikuchi, "Three-dimensional analysis of RF electromagnetic field by finite element method," *IEEE Trans. Magn.*, vol. MAG-19, pp. 2417–2420, Nov. 1983.

[10] J. P. Webb, "The finite-element method for finding modes of dielectric-loaded cavities," *IEEE Trans. Microwave Theory Tech.*, vol. MTT-33, pp. 635–639, July 1985.

[11] W. Wilhelm, "CAVIT and CAV3D-computer programs for RF

cavities with constant cross section or any three-dimensional form," *Part. Accel.*, vol. 12, pp. 139–145, 1982.
[12] L. Lewin, "Radiation from discontinuities in strip-line," *Proc. Inst. Elec. Eng.*, part C, pp. 163–170, Sept. 1960.
[13] H. Lee and V. K. Tripathi, "Spectral domain analysis of frequency dependent propagation characteristics of planar structures on uniaxial medium," *IEEE Trans. Microwave Theory Tech.*, vol. MTT-30, pp. 1188–1193, Aug. 1982.
[14] L. Lewin, "Spurious radiation from a microstrip Y junction," *IEEE Trans. Microwave Theory Tech.*, vol. MTT-26, pp. 893–894, Nov. 1978.
[15] I. V. Lindell, "Variational methods for nonstandard eigenvalue problems in waveguide and resonator analysis," *IEEE Trans. Microwave Theory Tech.*, vol. MTT-30, pp. 1194–1204, Aug. 1982.
[16] I. V. Lindell, "Asymptotic high-frequency modes of homogeneous waveguide structures with impedance boundaries," *IEEE Trans. Microwave Theory Tech.*, vol. MTT-29, pp. 1087–1093, Oct. 1981.
[17] C. T. M. Chang, "Circular waveguides lined with artificial anisotropic dielectrics," *IEEE Trans. Microwave Theory Tech.*, vol. MTT-20, pp. 517–523, Aug. 1972.
[18] S. A. Kheifets, "Electromagnetic fields in an axial symmetric waveguide with variable cross section," *IEEE Trans. Microwave Theory Tech.*, vol. MTT-29, pp. 222–229, Mar. 1981.
[19] K. F. Casey, "On inhomogeneously filled rectangular waveguides," *IEEE Trans. Microwave Theory Tech.*, vol. MTT-21, pp. 566–567, Aug. 1973.
[20] A. Konrad and P. Silvester, "Triangular finite elements for the generalized Bessel equation of order m," *Int. J. Num. Meth. Engng.*, vol. 7, pp. 43–55, 1973.
[21] K. Halbach and R. F. Holsinger, "SUPERFISH—A computer program for evaluation of RF cavities with cylindrical symmetry," *Part. Accel.*, vol. 7, pp. 213–222, 1976.
[22] R. L. Gluckstern, R. F. Holsinger, K. Halbach, and G. N. Minerbo, "ULTRAFISH—Generalization of SUPERFISH to $m \geqslant 1$," in *Proc. Linear Accel. Conf.* (Santa Fe, NM), pp. 102–107, 1981.
[23] M. Couture, "A study on the use of the magnetic Hertz vector to calculate fields in cavities," Atomic Energy of Canada Limited Report AECL-9188, Sept. 1986.
[24] A. Nisbet, "Hertzian electromagnetic potentials and associated gauge transformations," *Proc. Roy. Soc.*, vol. 231A, pp. 250–263, Aug. 1955.
[25] A. Konrad, "Linear accelerator cavity field calculation by finite element method," *IEEE Trans. Nucl. Sci.*, vol. NS-20, pp. 802–808, Feb. 1973.
[26] A. M. Winslow, "Numerical solution of the quasilinear Poisson equation in a nonuniform triangle mesh," *J. Comput. Phys.*, vol. 2, pp. 149–172, Nov. 1966.
[27] K. C. D. Chan, "Comparison of frequencies calculated by URMEL to experimental data," Chalk River Nuclear Laboratories, unpublished.
[28] H. Herminghaus and H. Enteneuer, "Beam blowup in race track microtrons," *Nucl. Instrum. Methods*, vol. 163, pp. 299–308, 1979.
[29] Y. Iwashita, "Use of ULTRAFISH and comparison to measured results," Los Alamos National Lab. Tech. Memorandum AT-DO: 82-350, Oct. 18, 1982.
[30] C. S.. Biddlecombe, E. A. Heighway, J. Simkin, and C. W. Trowbridge, "Methods for eddy current computation in three dimensions," *IEEE Trans. Magn.* vol. MAG-18, pp. 492–497, Mar. 1982.
[31] N. Perrone and R. Kao, "A general finite difference method for arbitrary meshes," *Int. J. Computers and Struct.*, vol. 5, pp. 45–58, 1975.
[32] V. Pavlin and N. Perrone, "Finite difference energy techniques for arbitrary meshes applied to linear plate problems," *Int. J. Num. Meth. Engng.*, vol. 7, pp. 647–664, 1979.
[33] T. Liszka and J. Orkisz, "The finite difference method at arbitrary irregular grids and its application in applied mechanics," *Int. J. Computers and Struct.*, vol. 11, pp. 83–95, 1980.
[34] G. B. Denegri, G. Molinari, and A. Viviani, "A generalized finite difference method for the computation of electric and magnetic fields," in *Proc. COMPUMAG Conf.* (Oxford), Mar.–Apr. 1976.
[35] G. Molinari, M. R. Podesta, G. Sciutto, and A. Viviani, "Finite difference method with irregular grid and transformed discretization metric," presented at IEEE PES Winter Meeting, New York, paper A78 288-3, Jan. 1978.
[36] P. Molfino, G. Molinari, and A. Viviani, "A user-oriented modular package for the solution of general field problems under time varying conditions," *IEEE Trans. Magn.*, vol. MAG-18, pp. 638–643, Mar. 1982.
[37] M. Cena, P. Fernandez, E. Furnari, and R. Parodi,, "Least square treatment of boundary conditions in FDM programs with regular meshes," *IEEE Trans. Magn.* vol. MAG-21, pp. 2519–2522, Nov. 1985.
[38] P. Girdinio, P. Molfino, G. Molinari, and A. Viviani, "A package for computer aided design for power electrical engineering," *IEEE Trans. Magn.* vol. MAG-19, pp. 2659–2662, Nov. 1983.
[39] P. R. Kotiuga and P. P. Silvester, "Vector potential formulation for three-dimensional magnetostatics," *J. Appl. Phys.*, vol. 53, pp. 8399–8401, Nov. 1982.
[40] O. A. Mohammed, W. A. Davis, B. D. Popovic, T. W. Nehl, and N. A. Demerdash, "On the uniqueness of solution of magnetostatic vector-potential problems by three-dimensional finite-element methods," *J. Appl. Phys.*, vol. 53, pp. 8402–8404, Nov. 1982.

✠

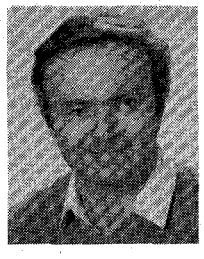

Michel Couture received the B.Sc. degree (with honors) in physics from the Collège Militaire Royal de St. Jean (Canada) in 1971. He served with the Royal Canadian Air Force from 1966 to 1976. He received the M.Sc. and Ph.D. degrees from McGill University in 1975 and 1980, both in theoretical physics.

He has been with the Theoretical Physics Branch of the Chalk River Nuclear Laboratories since 1980.